COMPARISON OF GIANT RADIO PULSES IN YOUNG AND MILLISECOND PULSARS

Aga Słowikowska (MPE, CAMK)

Axel Jessner (MPIfR)

Gottfried Kanbach (MPE)

Bernd Klein (MPIfR)

363rd Heraeus Seminar

Neutron Stars and Pulsars

May 15, 2006

The intriguing phenomenon of Giant Radio Pulses in pulsars

- Main Features of GRPs
- The Crab pulsar case
- Our observations: discovery of GRPs at its HFCs phases
- The millisecond pulsars
- Conclusions

Main Features of GRPs

- Strong pulses (> 10 x average) with power-law distribution
- No evidence for a break of the power-law tail at high intensities, long observations would reveal the pulses of even higher intensities
- Low intensities, noise is significant, no direct evidence if GRPs form a separate group or whether there is a smooth transition from normal to GPs

Main Features of GRPs (part 2)

- Power-law index of GPs distribution differs markedly for different pulsars and depends on radio frequency
- For a given pulsar, GPs constitute only a tiny fraction of the total of pulses ($< 1\%$)
- They do not affect the average radio emission characteristics
- Usually fast rise and exponential decay, narrower than a normal pulse, the strongest one tending to be the narrowest
- Highly polarized (Crab – linearly, PSR B1937+21 circularly)

Detection of strong inter pulses (IP) from NP 0532

Sporadic giant pulses from the Crab Nebula were reported in the discovery paper on NP 0532 (Staelin & Reifenstein 1968) before a periodicity for the pulsar was established. Since then giant pulses have been observed at frequencies between 73.8 and 430 MHz by Staelin & Sutton 1970, Heiles, Campbell & Rankin 1970, Heiles and Rankin 1971.

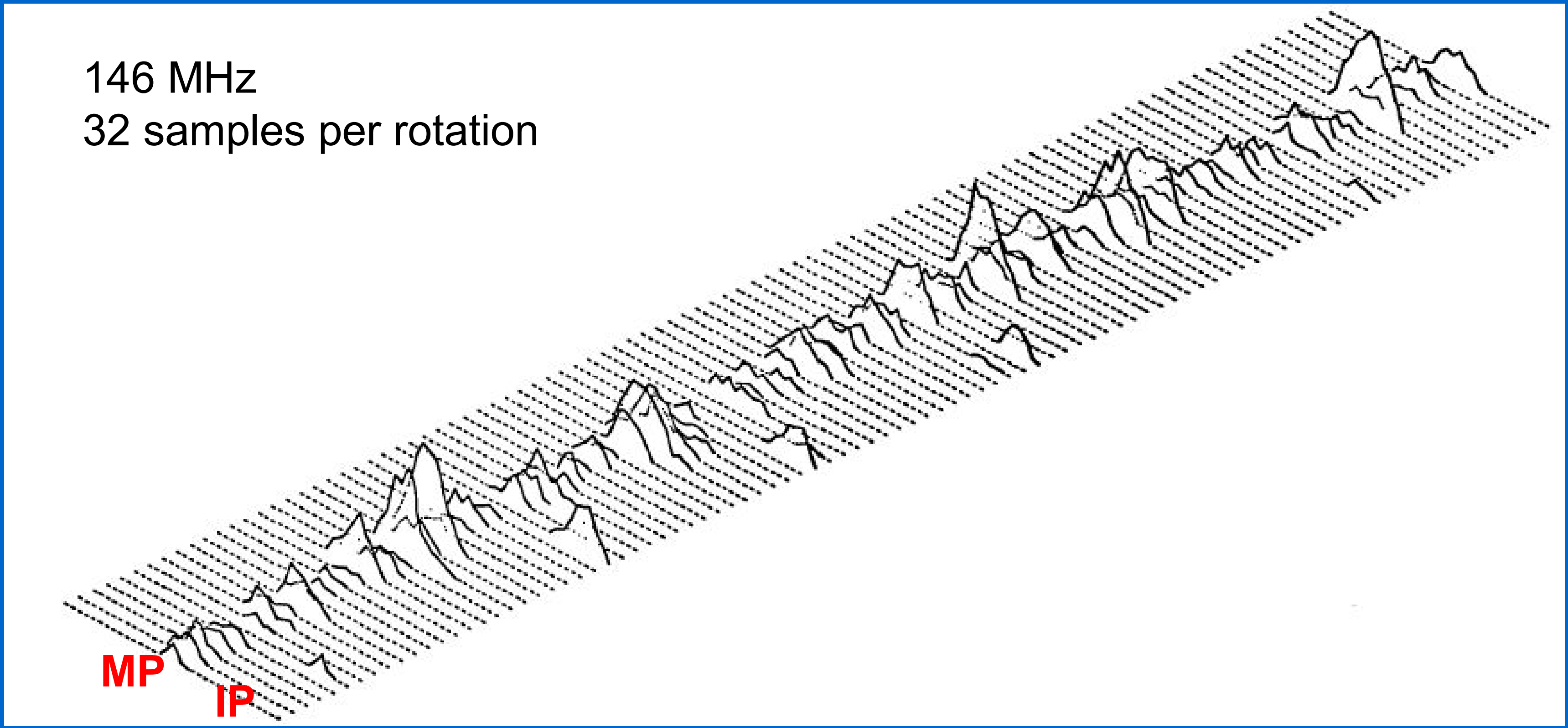

Seven giant inter pulses are visible in this 3-dimensional plot representing 4 hours' observation of NP 0532 at 146 MHz (Gower & Agryle 1972).

Statistics of giant pulses from NP 0532

Observations of NP 0532 at 146 MHz show that the sporadic giant pulses are associated with the inter pulse as well as with the main pulse. Roughly 8% of the strong pulses occur at the time of inter pulse, and the remaining 92% are associated with the main pulse (Gower & Argyle 1972).

$N = k * S^{\alpha}$

for MP $\alpha = -2.5$

for IP $\alpha = -2.8$

Argyle & Gower 1972

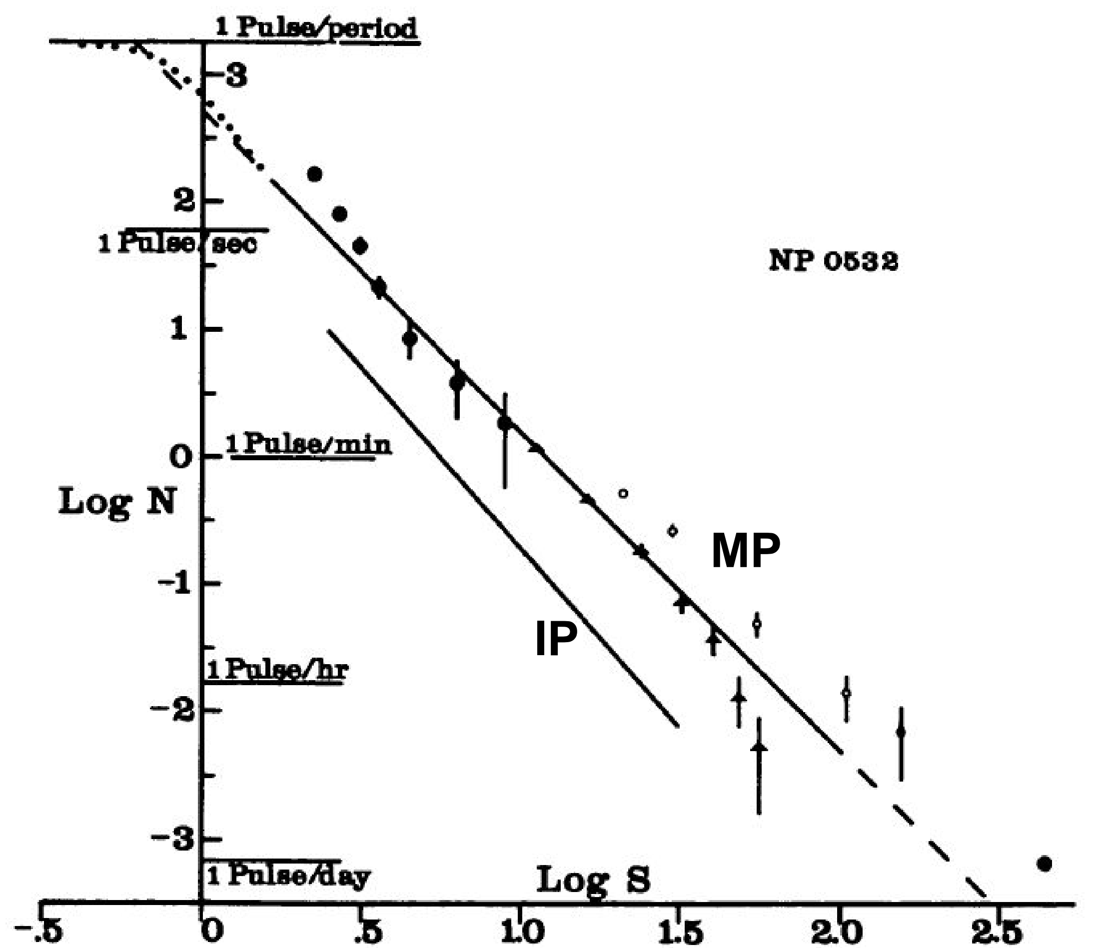

Radio profiles of the Crab pulsar between 0.8 and 8.4 GHz

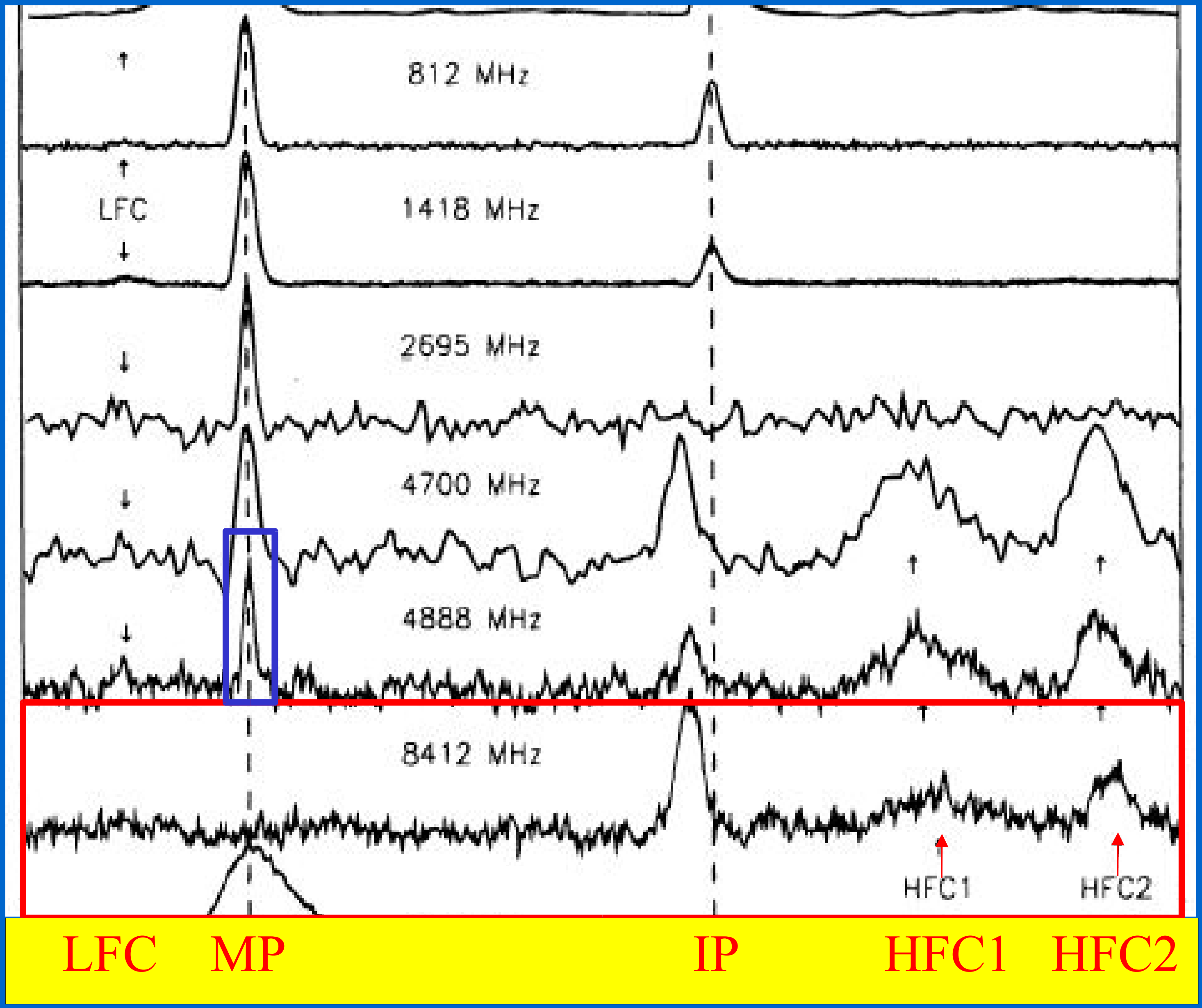

Moffett & Hankins, 1996

Train of strong giant pulses at 8.35 GHz, 100-m Effelsberg telescope

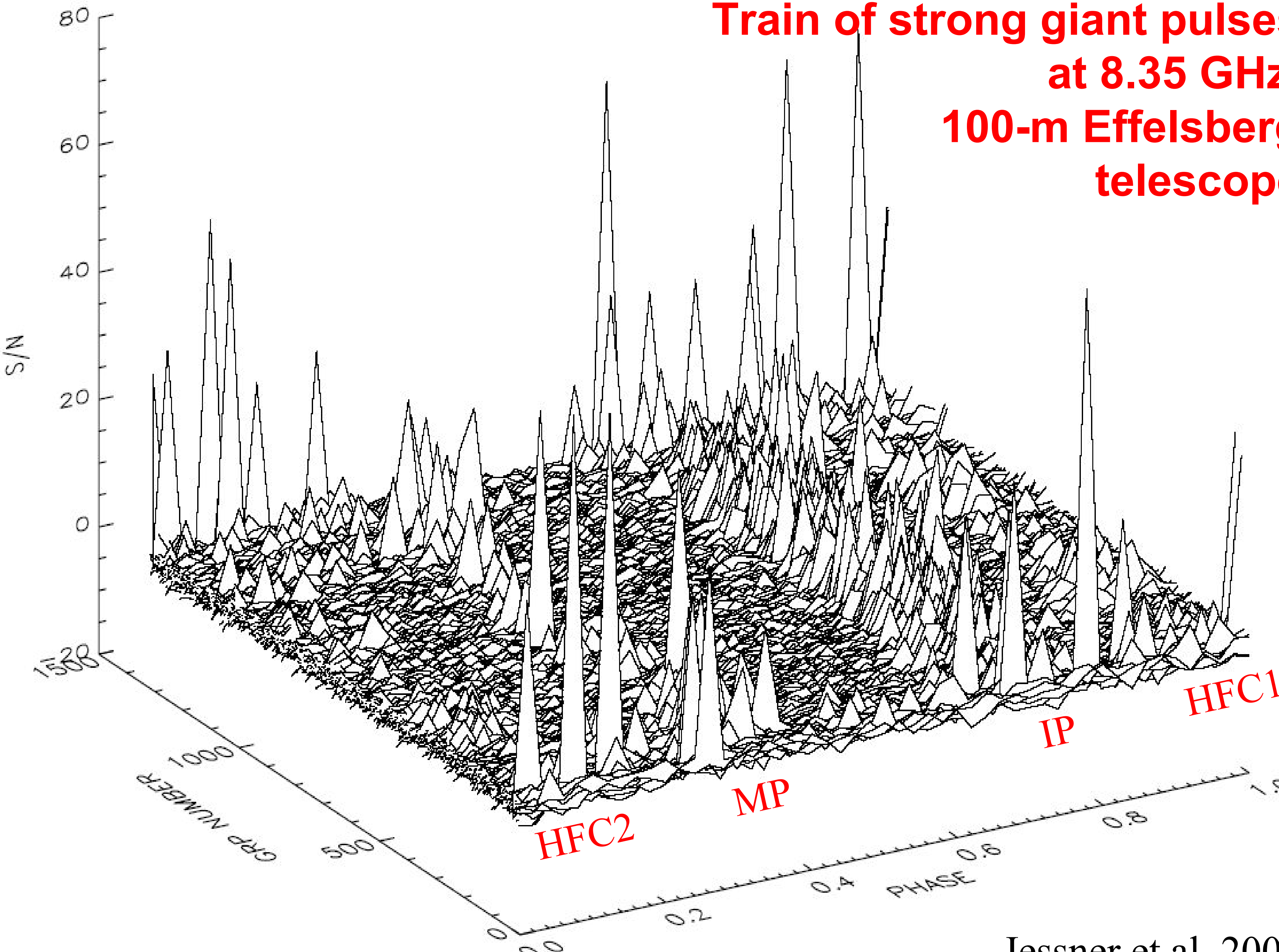

Jessner et al. 2005

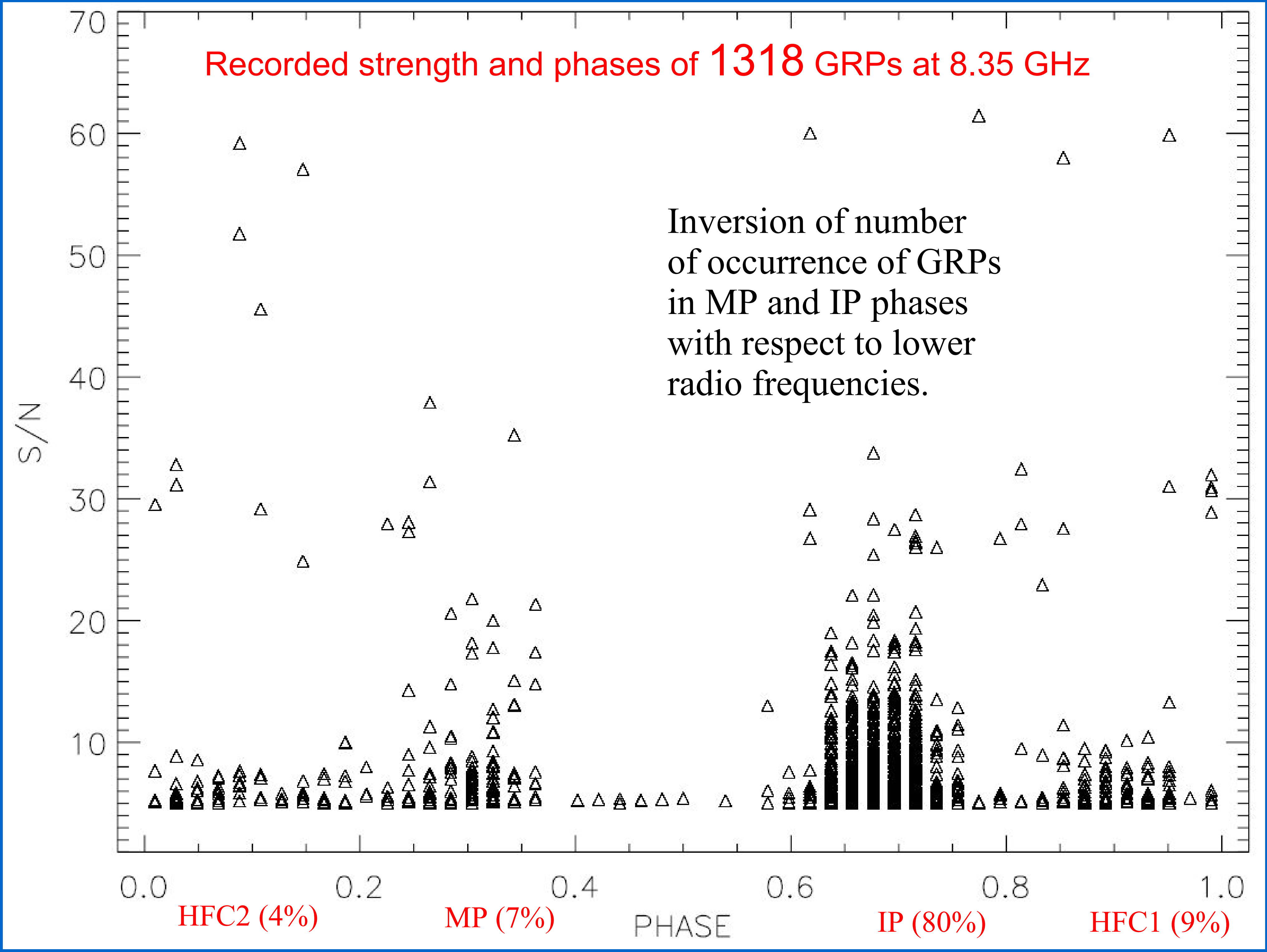

Recorded strength and phases of 1318 GRPs at 8.35 GHz
Inversion of number of occurrence of GRPs in MP and IP phases with respect to lower radio frequencies.
S/N
70
60
50
40
30
20
10
0.0
0.2
0.4
0.6
0.8
1.0
PHASE
HFC2 (4%)
MP (7%)
IP (80%)
HFC1 (9%)

Crab GRPs distribution

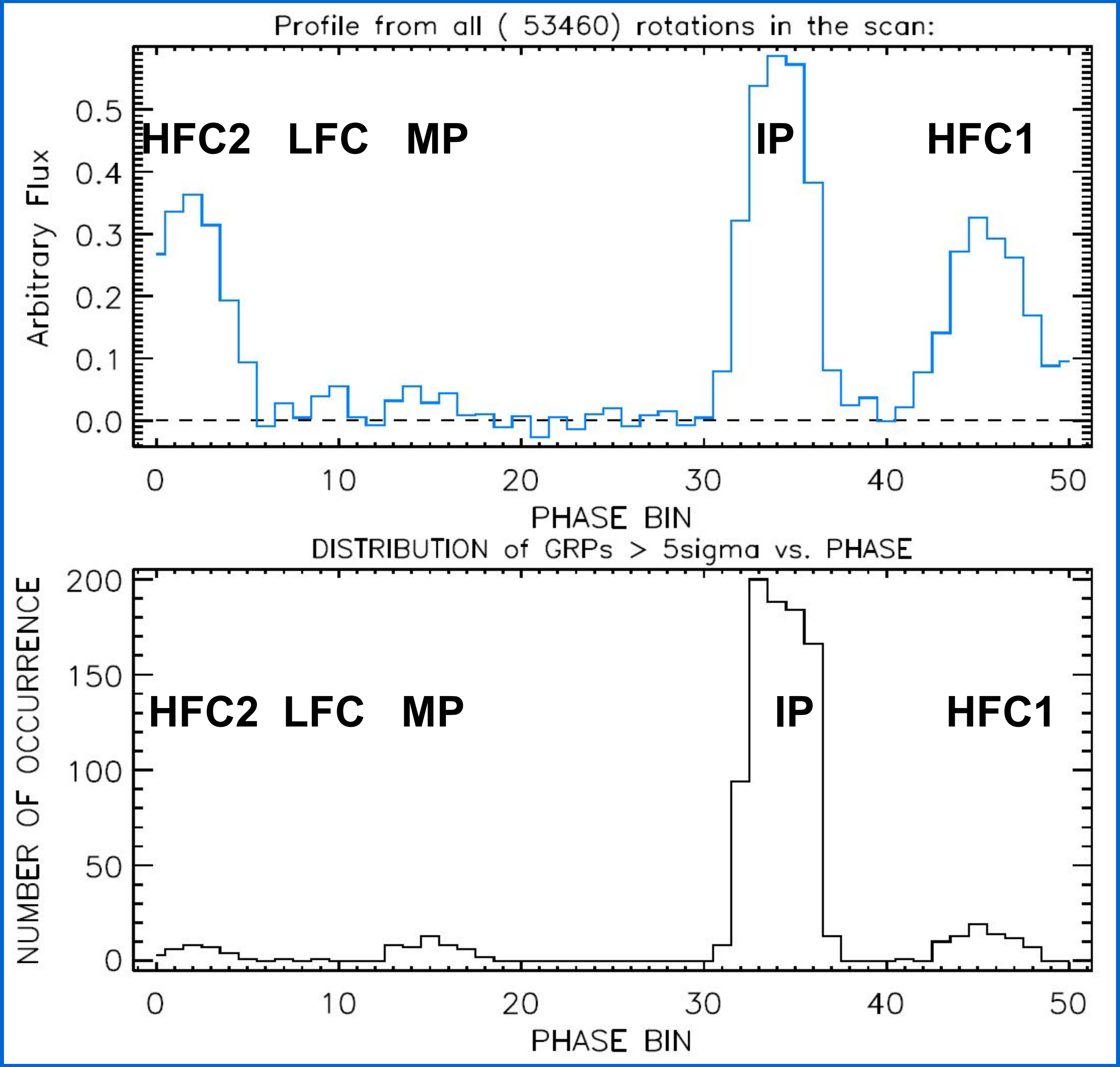

Słowikowska et al. 2006

Single Crab GRPs

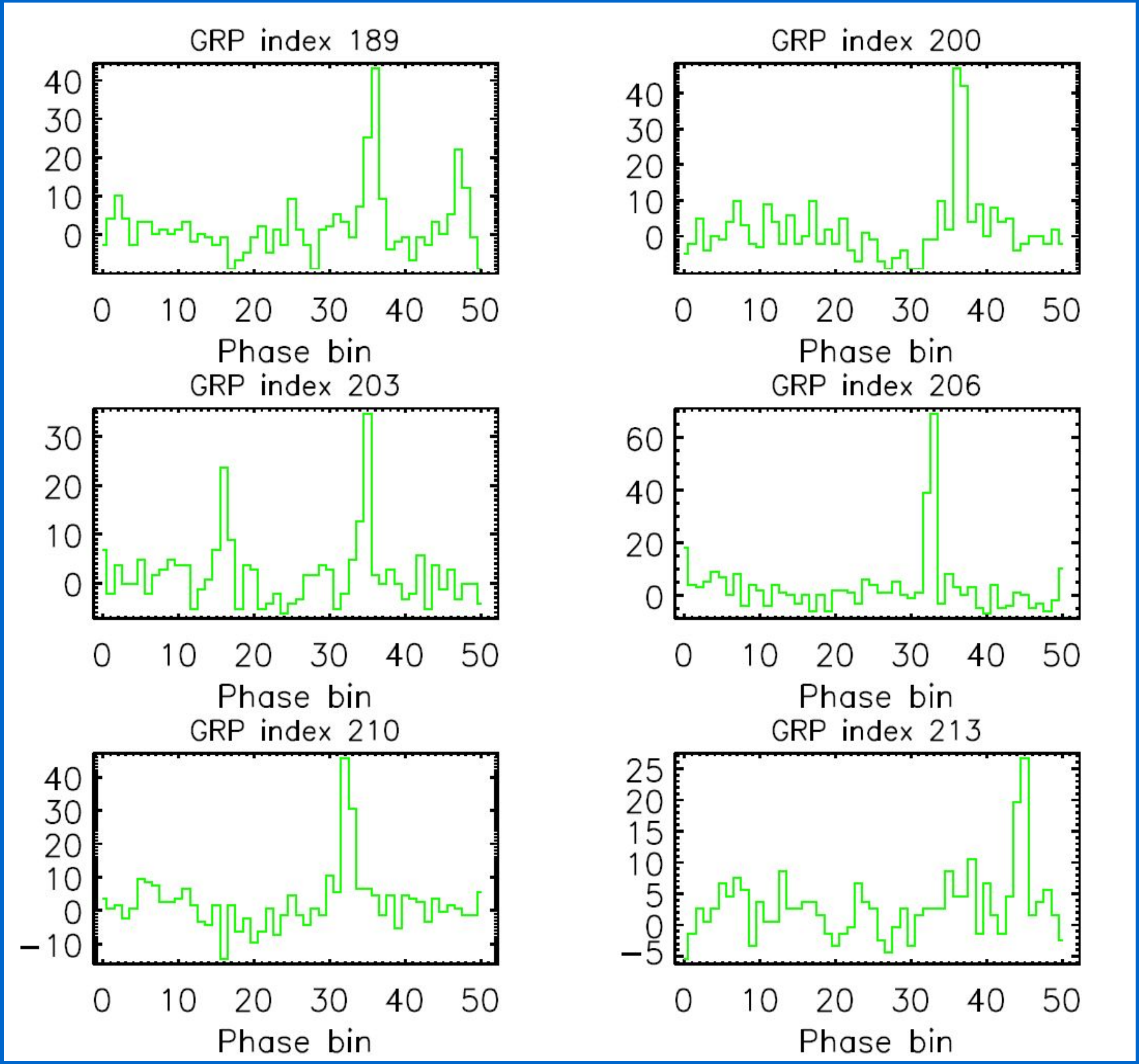

Słowikowska et al. 2006

Single Crab GRPs

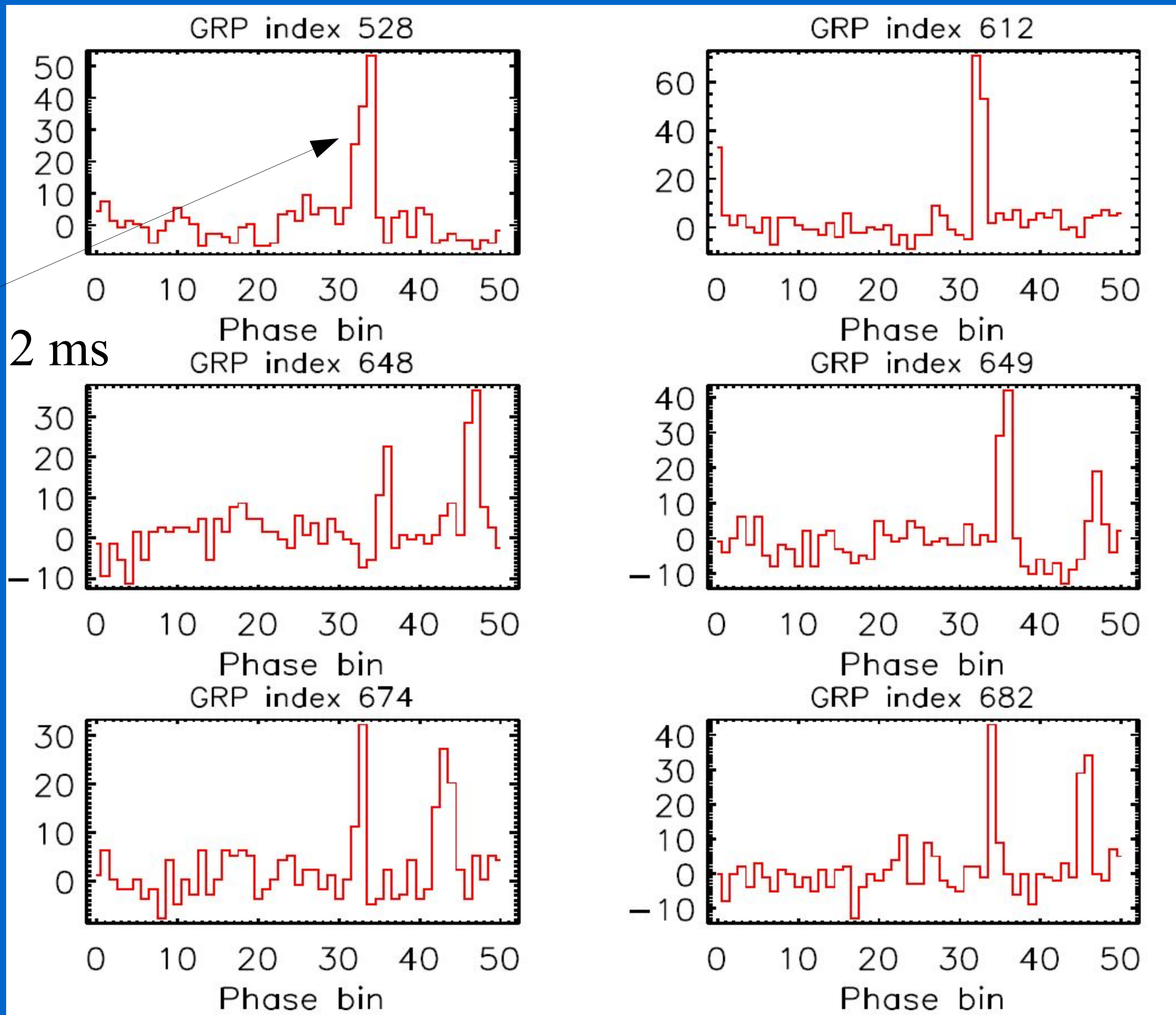

740 μs < τ < 2 ms

Słowikowska et al. 2006

Peak strength distribution of all GRPs at 8.35 GHz

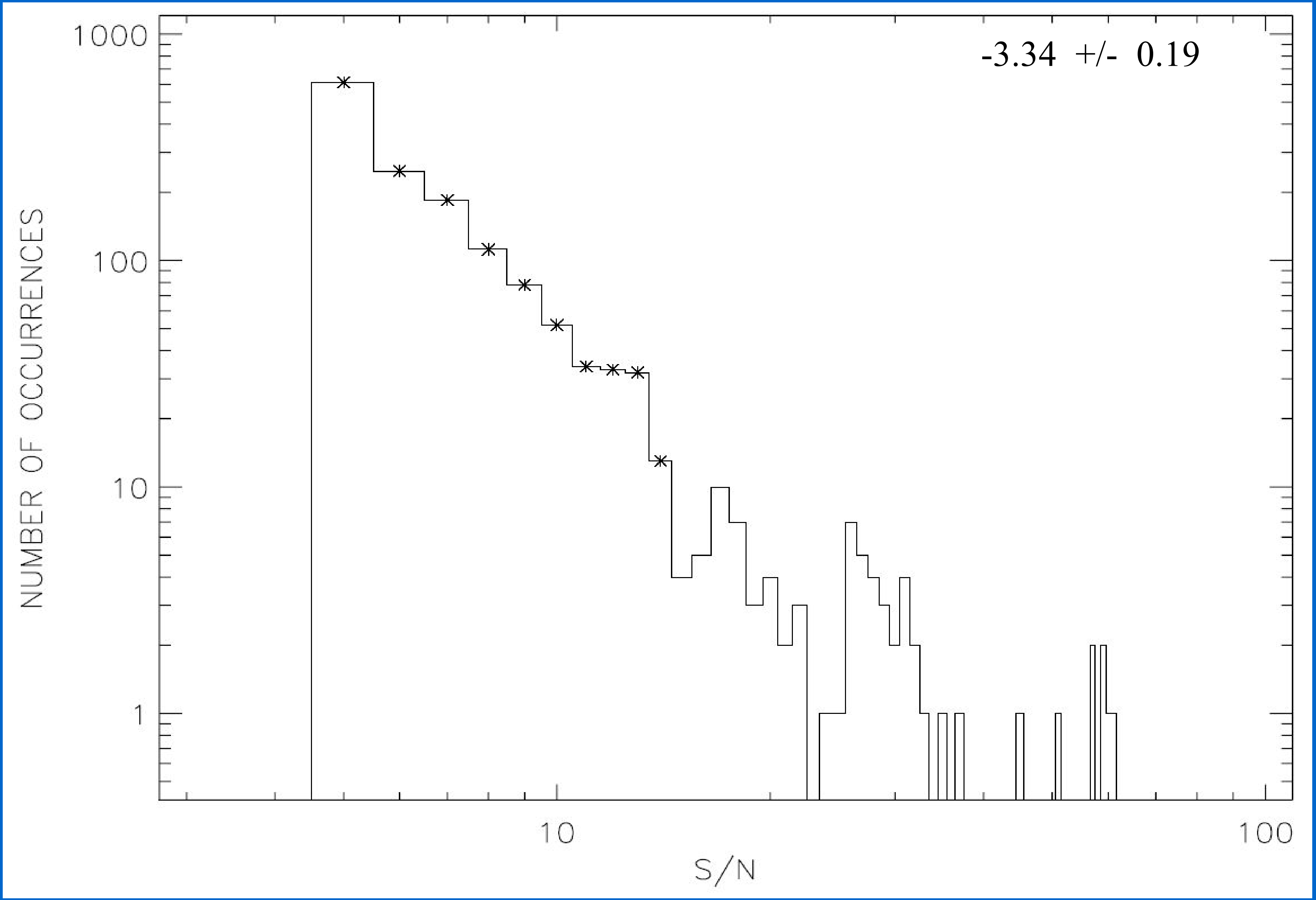

(0.812 GHz -3.5 Lundgren et al. 1995)

High Frequency Components (HFC1 and HFC2)

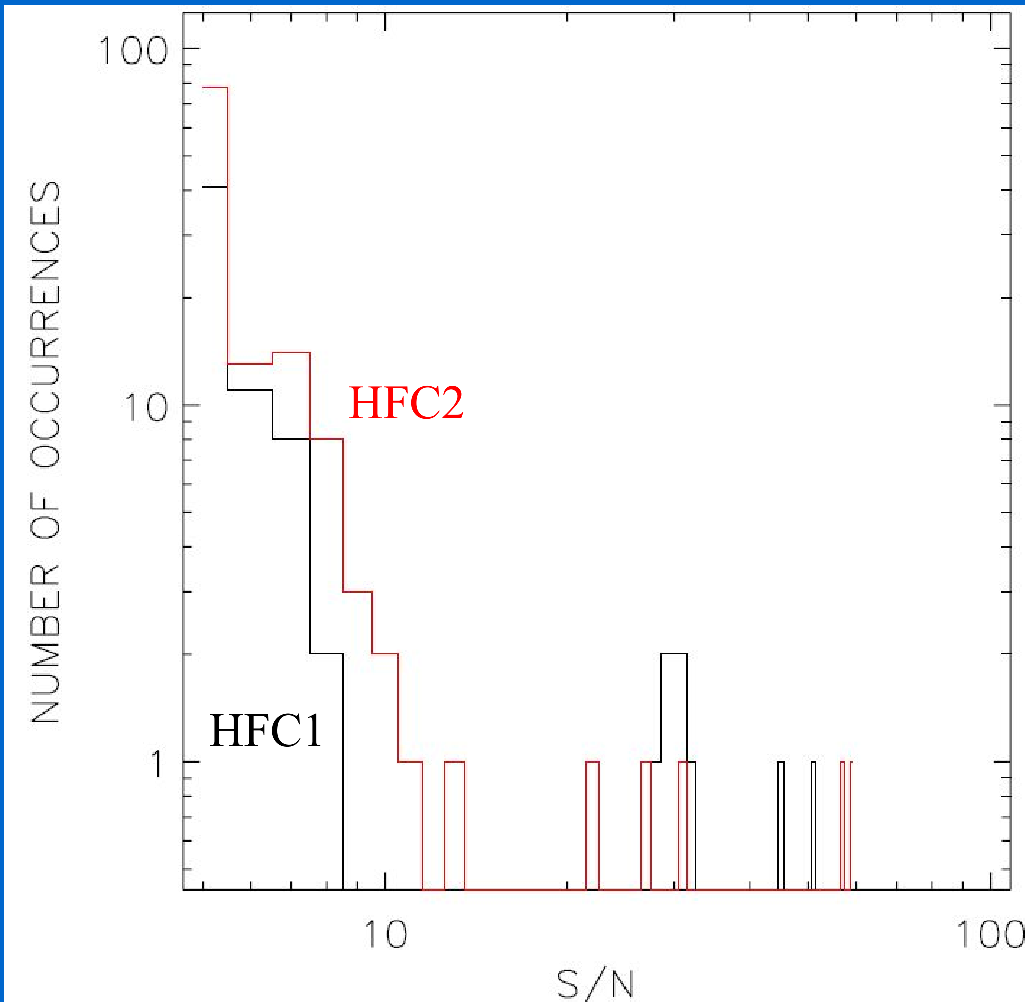

Jessner et al. 2005

Phase resolved peak strength distribution of GRPs at 8.35 GHz

Main Pulse (MP) and Inter Pulse (IP)

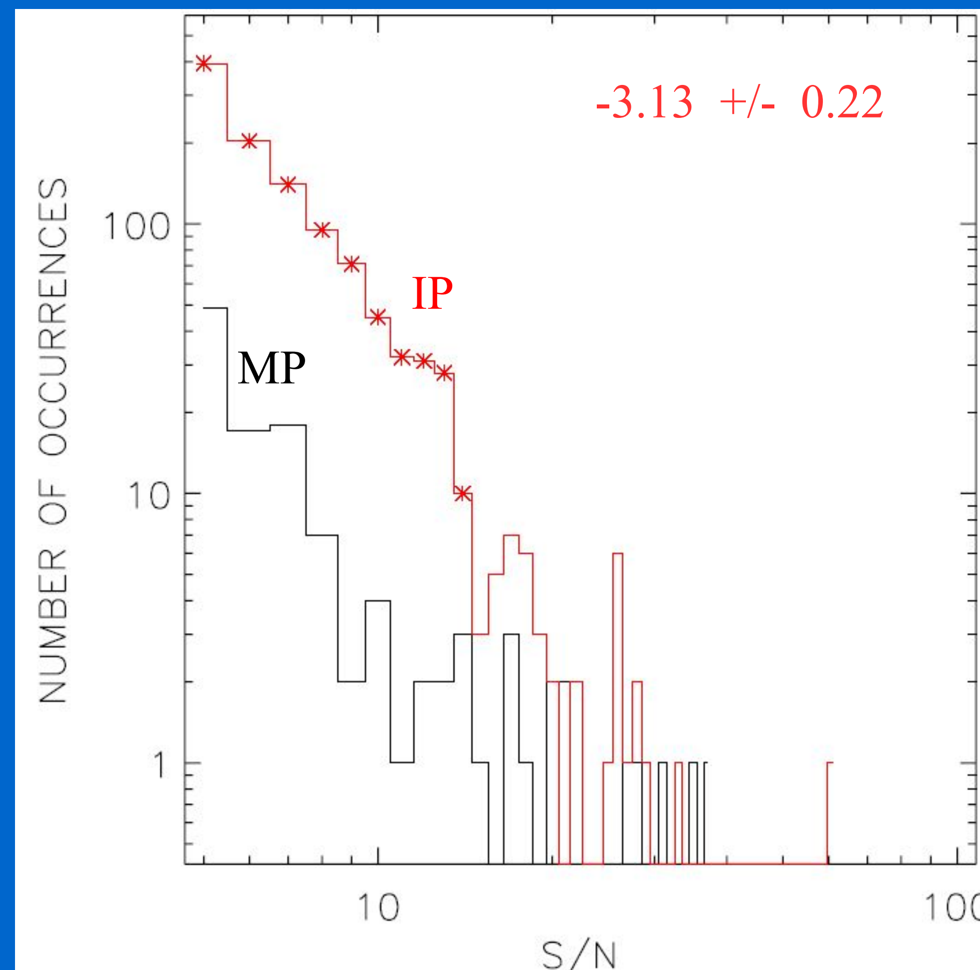

0.146 GHz -2.5 MP (Argyle & Gower 1972)
0.146 GHz -2.8 IP (Argyle & Gower 1972)
8.8 GHz -2.9 IP (Cordes et al. 2004)

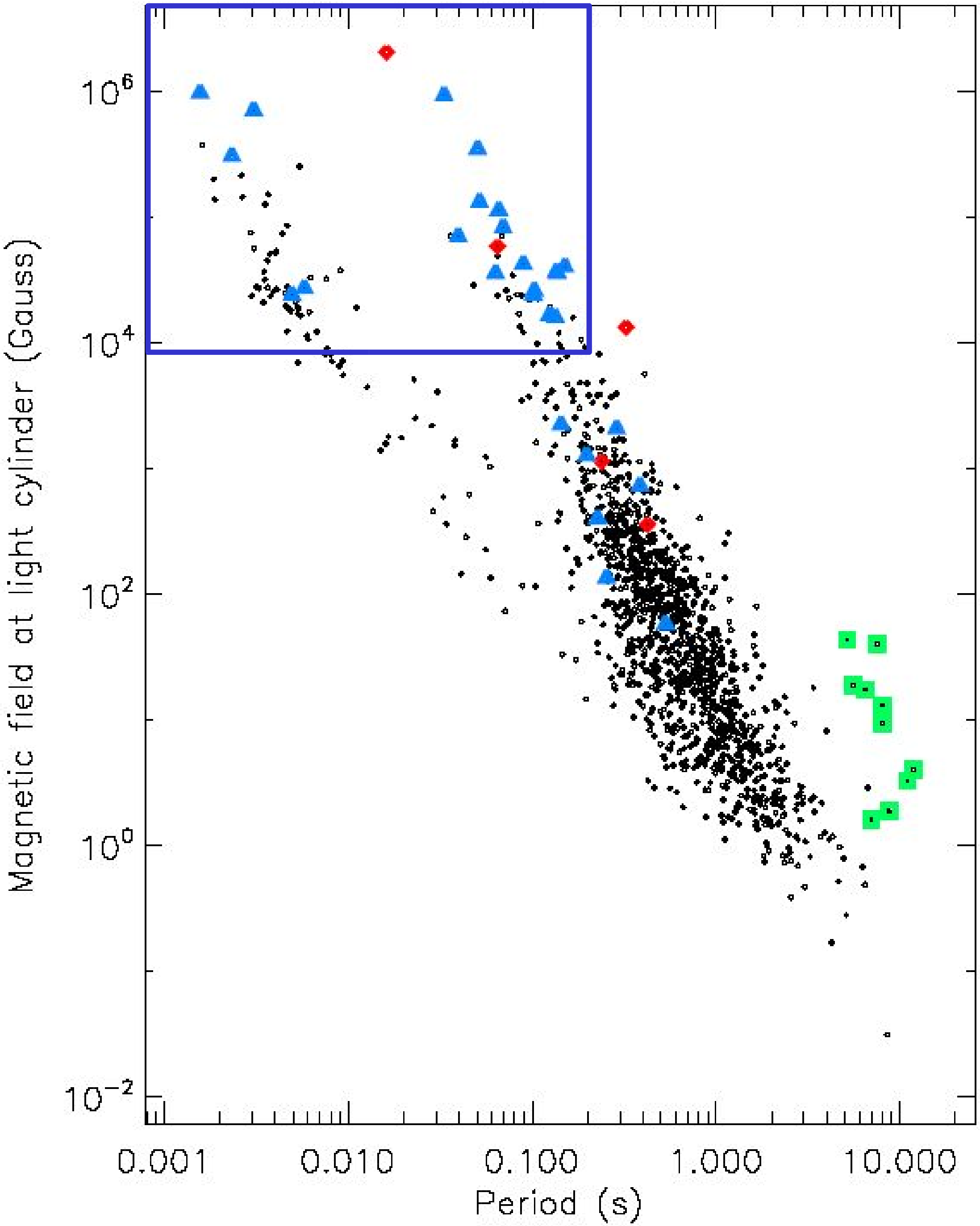

P – B_{LC} diagram;

$$B_{LC} = B_S (R_{NS}/R_{LC})^3 = 3 \cdot 10^8 \cdot P^{-5/2} \cdot \dot{P}^{1/2}$$

$R_{LC} = c\,P / 2\pi$

P = 1.558 ms	$R_{LC} \approx 7.4\ R_{NS}$
P = 33 ms	$R_{LC} \approx 158\ R_{NS}$
P = 0.1 s	$R_{LC} \approx 477\ R_{NS}$
P = 1.0 s	$R_{LC} \approx 4774\ R_{NS}$

R_{NS} = 10 km

Anomalous X-ray Pulsar or Soft Gamma-ray Repeater with pulsations

Spin-powered pulsars with pulsed emission in radio plus HE

Spin-powered pulsar with pulsed emission only at HE

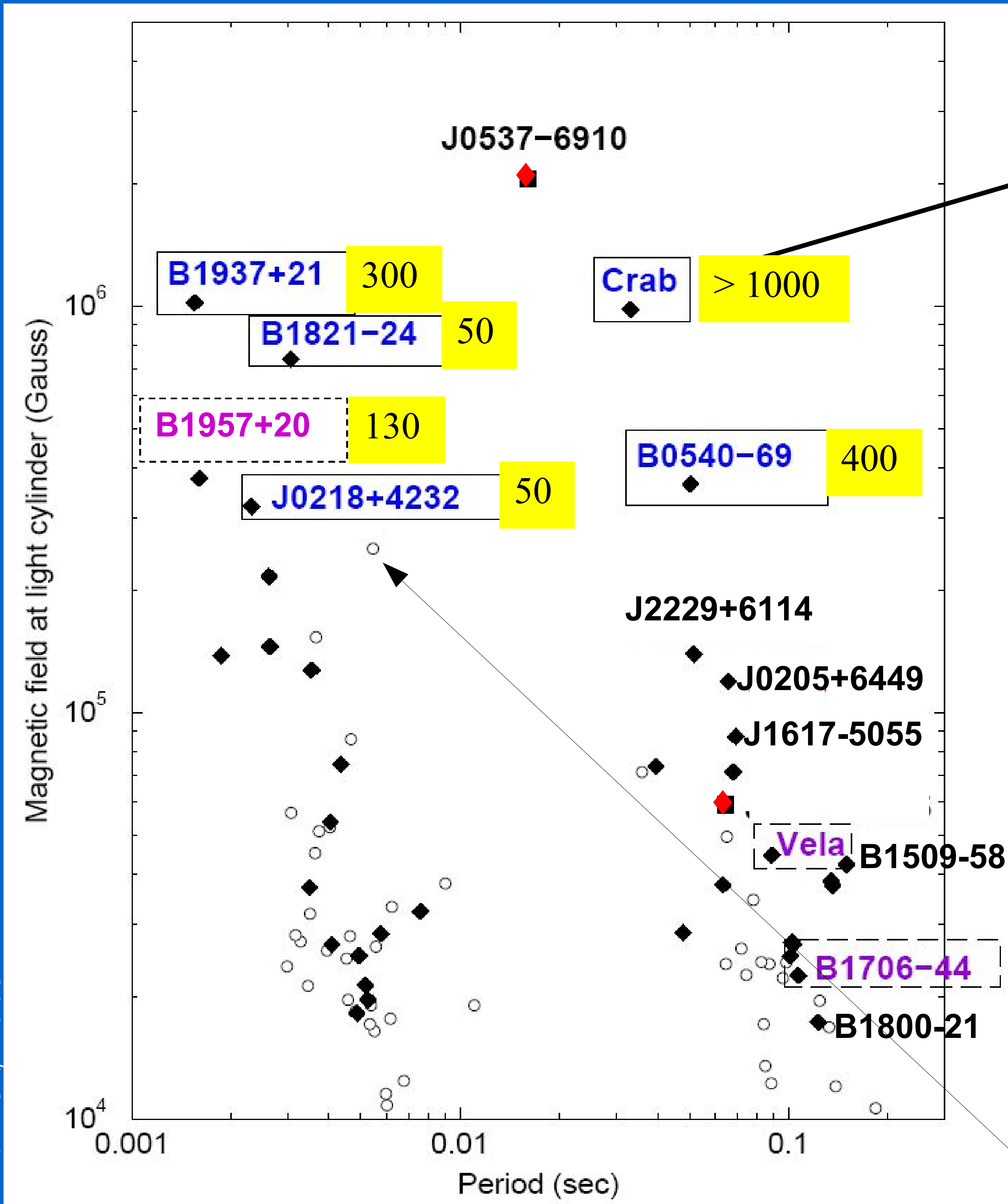

Kramer, 2003

The known emitters of GRPs

Biggest observed GRP
[unit of average pulse strength]

PSR B1133+16
(Kijak et al. 2006) 50 x mean

PSR J1823-3021A
(Knight et al. 2005) 64 x mean

Discovery of the first extragalactic giant radio pulses from PSR B0540-69

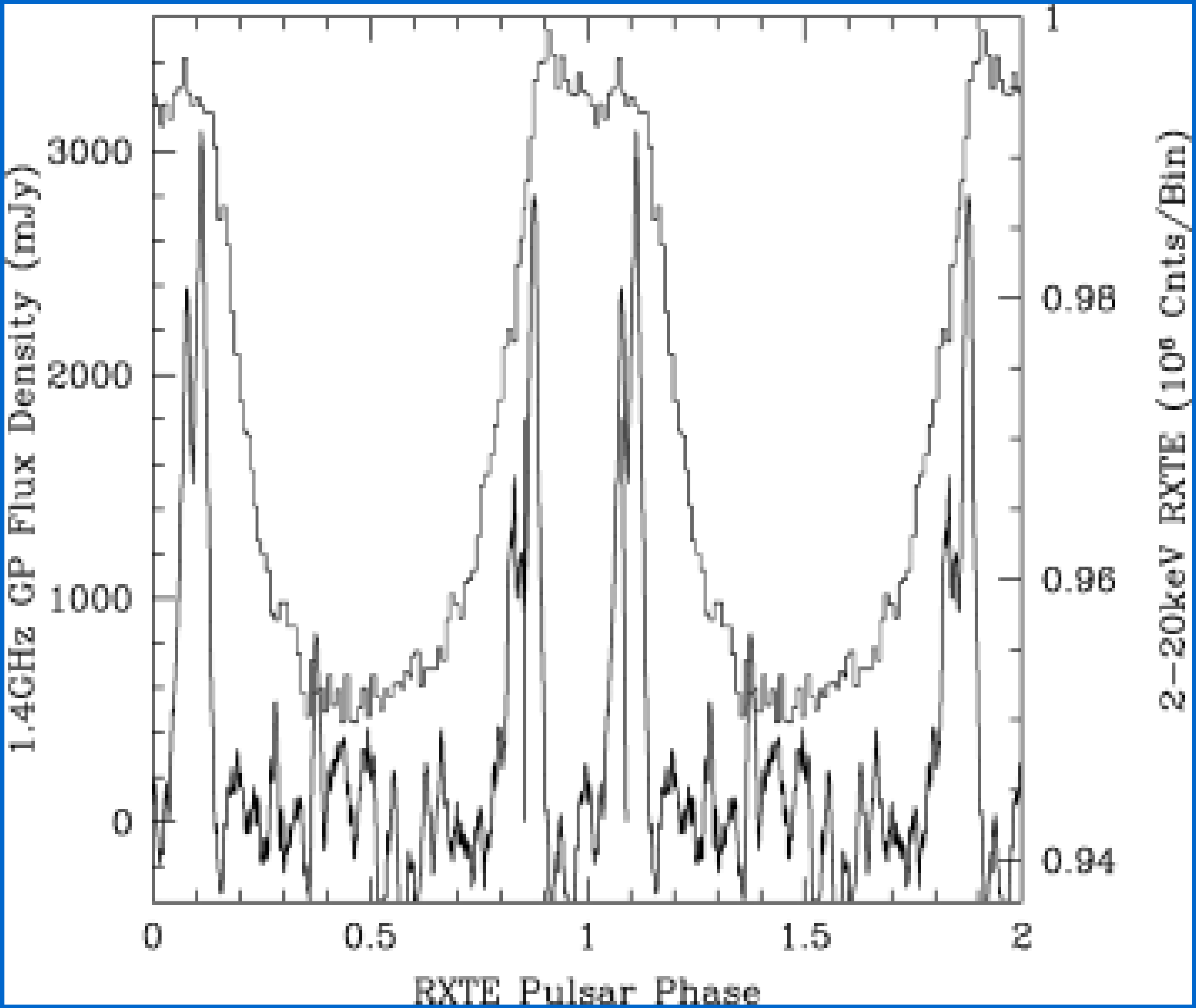

Johnston et al., MNRAS, 355, 2004

X-ray profiles

(70% of MSPs in binary systems, all MSPs known to emit giant pulses are solitary)

‘Crab-like’ MSPs with

high X-ray luminosities, hard spectra and narrow pulses

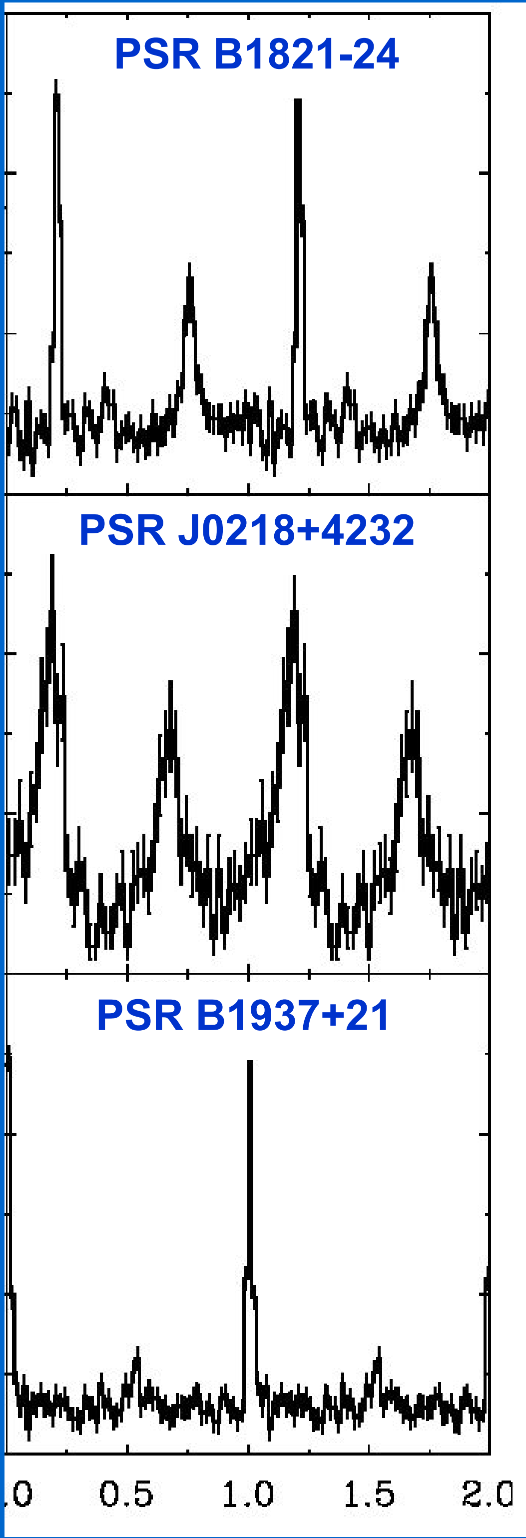

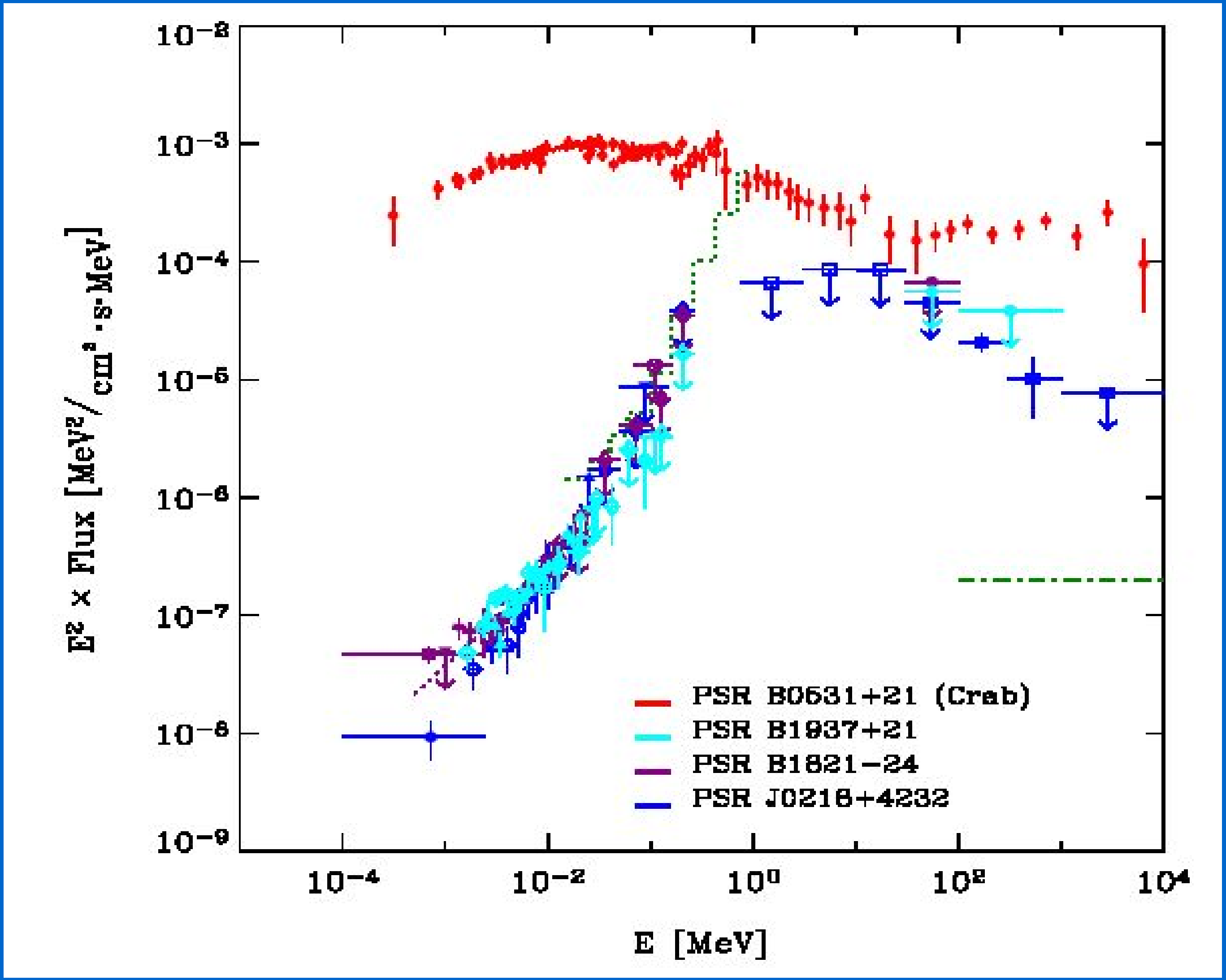

Kuiper & Hermsen, 2003

GRPs from PSR B1937+21

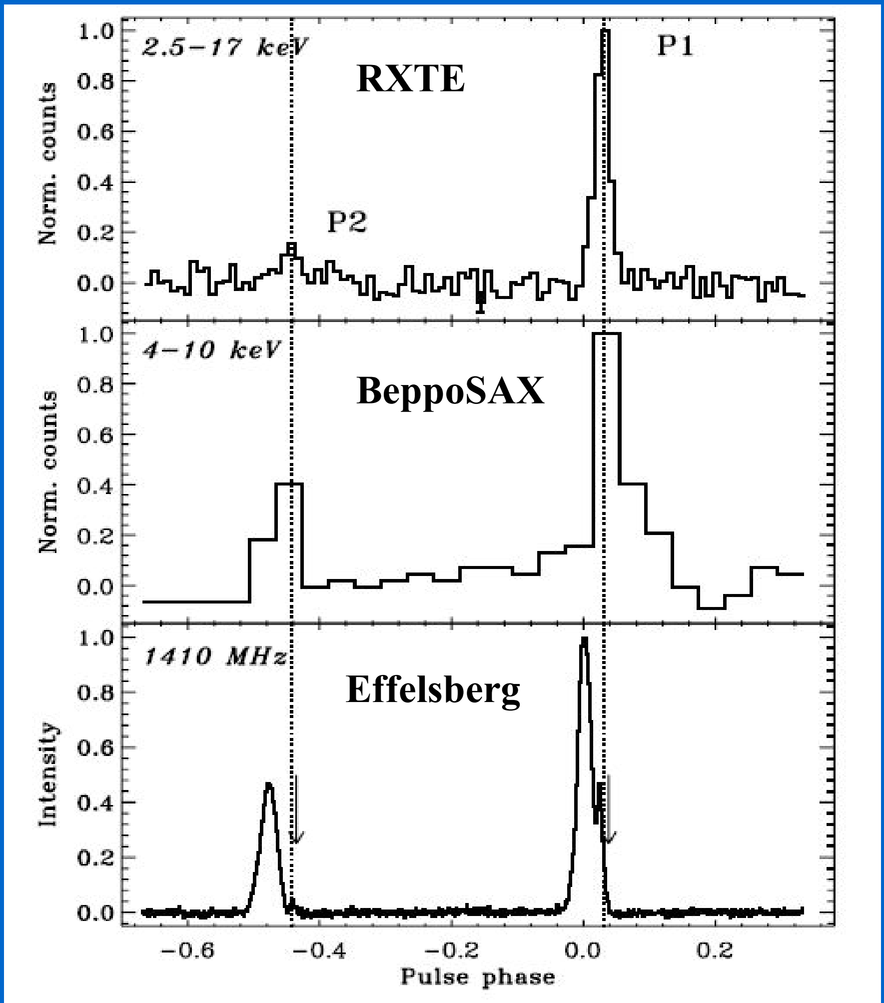

Cusumano et al. 2003

- GPs are not coincident with the peak of average radio pulse, but instead are in narrow ~1 degree phase windows on the extreme outer trailing edge of each of the main and inter pulse region (P1 lags the MP by 44 μs, P2 lags the IP by 51 μs (confirmed by Soglasnov et al. 2004, 58 μs and 65 μs, respectively)
- Power-law index of the intensity distribution α=-1.8+/-0.1 Cognard et al. 1996, α= -1.4 Soglasnov et al. 2004

GRPs from PSR B1821-24

P1 lags the integrated FP by 80 μs

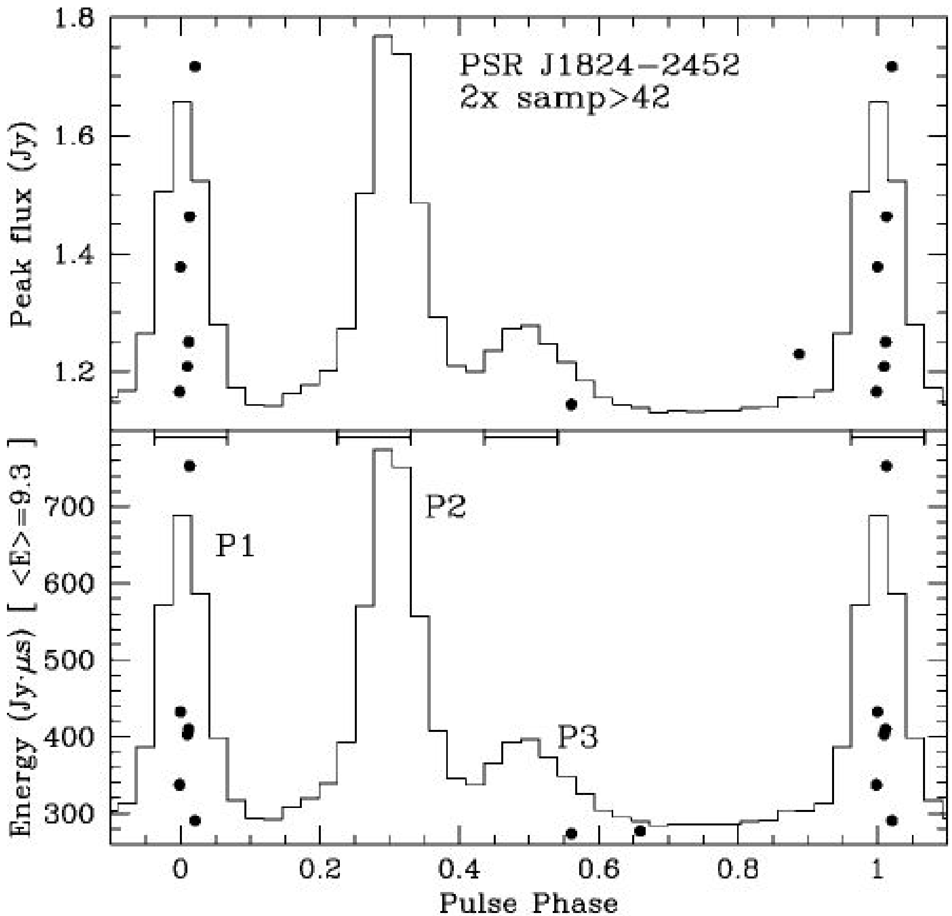

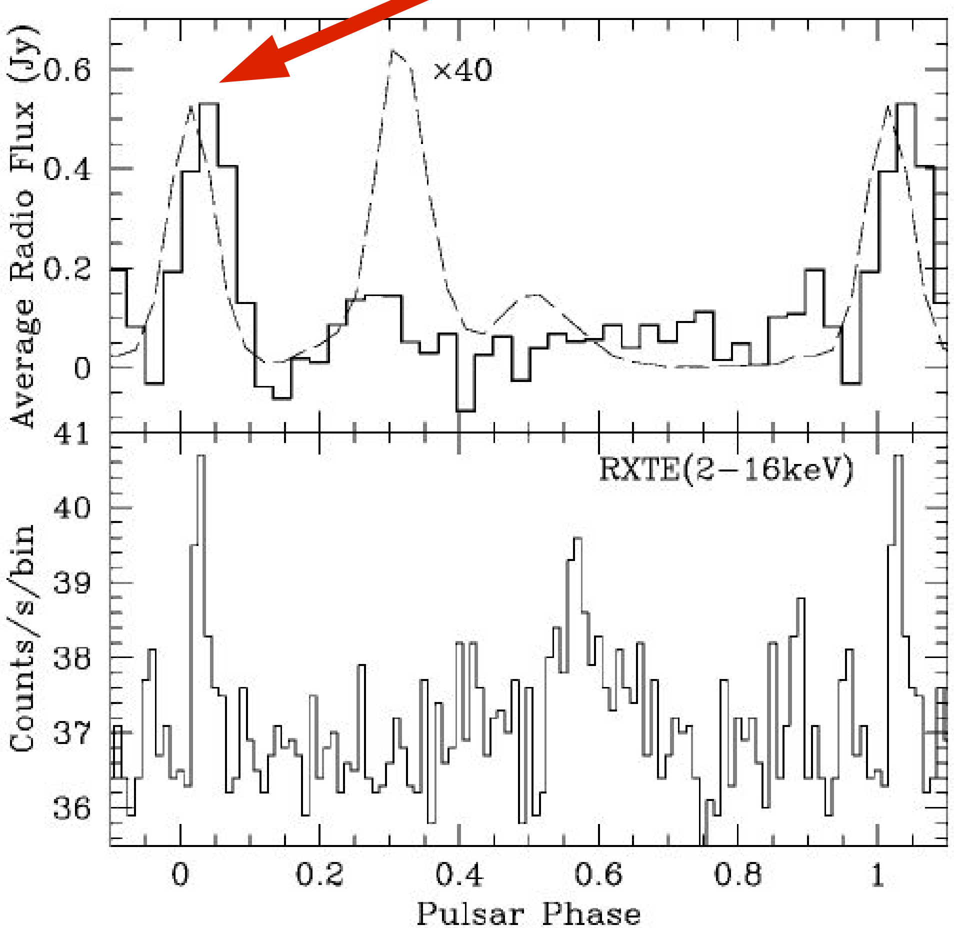

GRPs from the gamma-ray MSP, J0218+4232

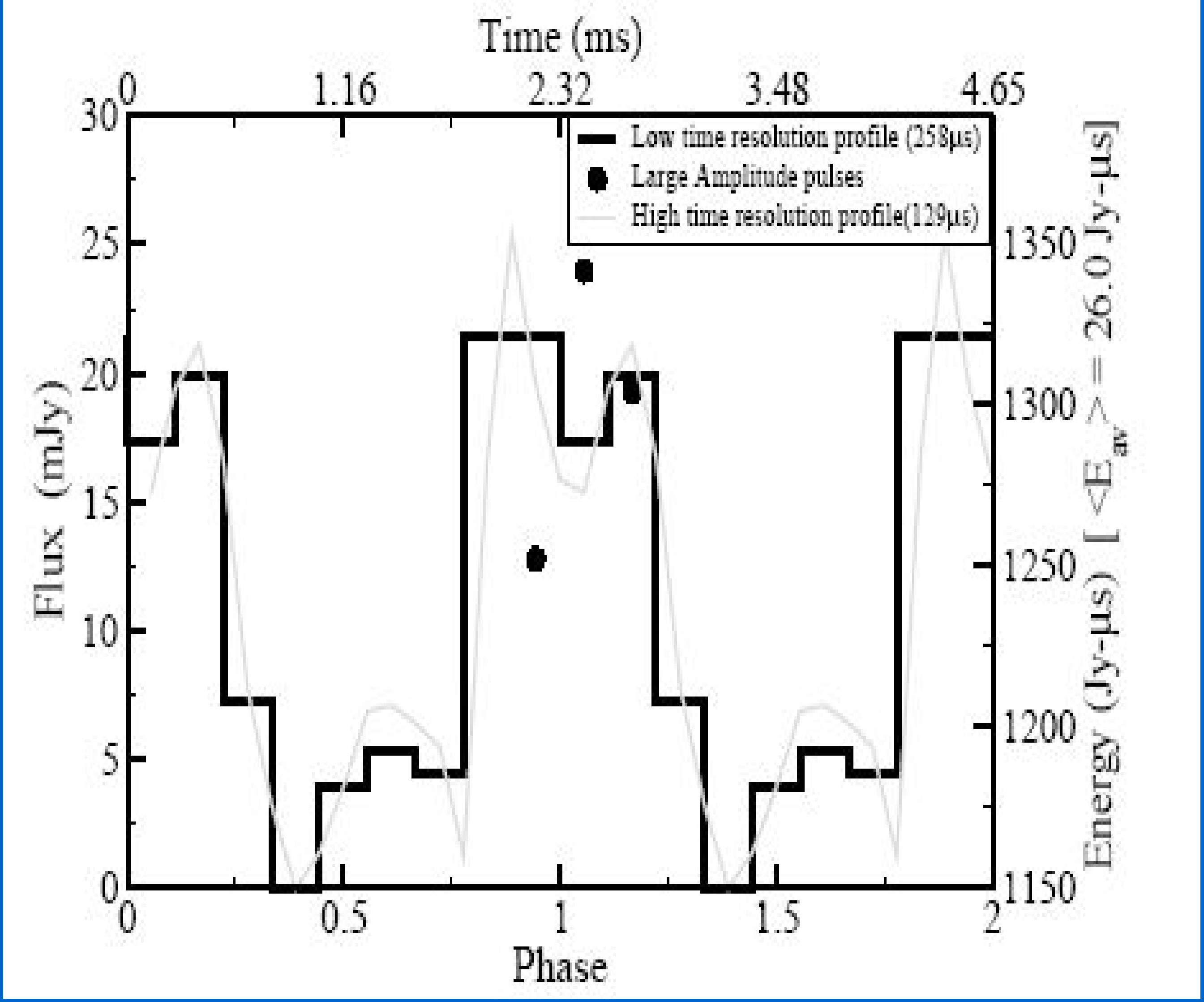

3 GRPs per
2.2 x 10^6 rotations
max: 51 x mean
int ~ 1341 Jy-μs

Joshi et al., 2003

Conclusions

Giant Radio Pulses are a phenomenon observed for classical and millisecond Crab-like pulsars with strong magnetic field at the light cylinder.

There is growing evidence that GRPs are tracers of high-energy (i.e. Optical, X-ray and Gamma-ray) activity of those pulsars.

We have discovered GRPs of the Crab pulsar at high frequency (8.35 GHz) occuring at all phases (MP, IP, HFCs).

The origin of HFCs is unknown. The outer gap model suggests that they might come from inward moving particles.

The three MSPs that are known to emit GRPs have the highest spin-down luminosity, therefore dE/dt rather than B_LC may be a better indicator of GP emission for MSPs.

New high-quality multiwavelength observations (sensitive single-pulse studies) are necessary to foster theoretical work on the nature of GRPs and HFCs.

Crab chronology

- discovery of dispersed pulse signals from the Crab Nebula - Staelin & Reifenstein 1968
- period and other properties where measured by Comella et al. 1969
- slowdown rate of NP 0532 – Richards & Comella 1969
- optical emission was reported by Cocke, Disney & Taylor, 1969
- detection at hard X-rays – Fishman et al. 1969
- detection at soft X-rays – Boldt et al. 1969; Fritz et al. 1969
- detection at infrared wavelengths Neugebauer et al. 1969
- ...

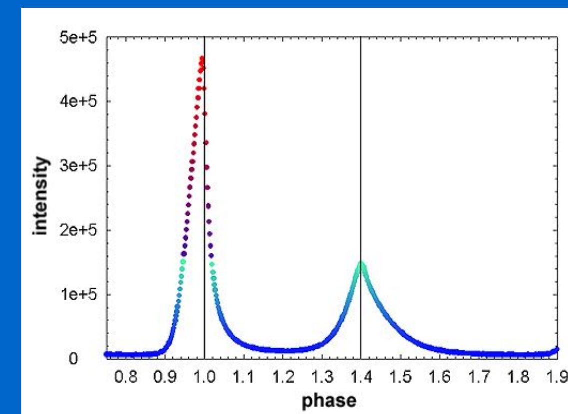

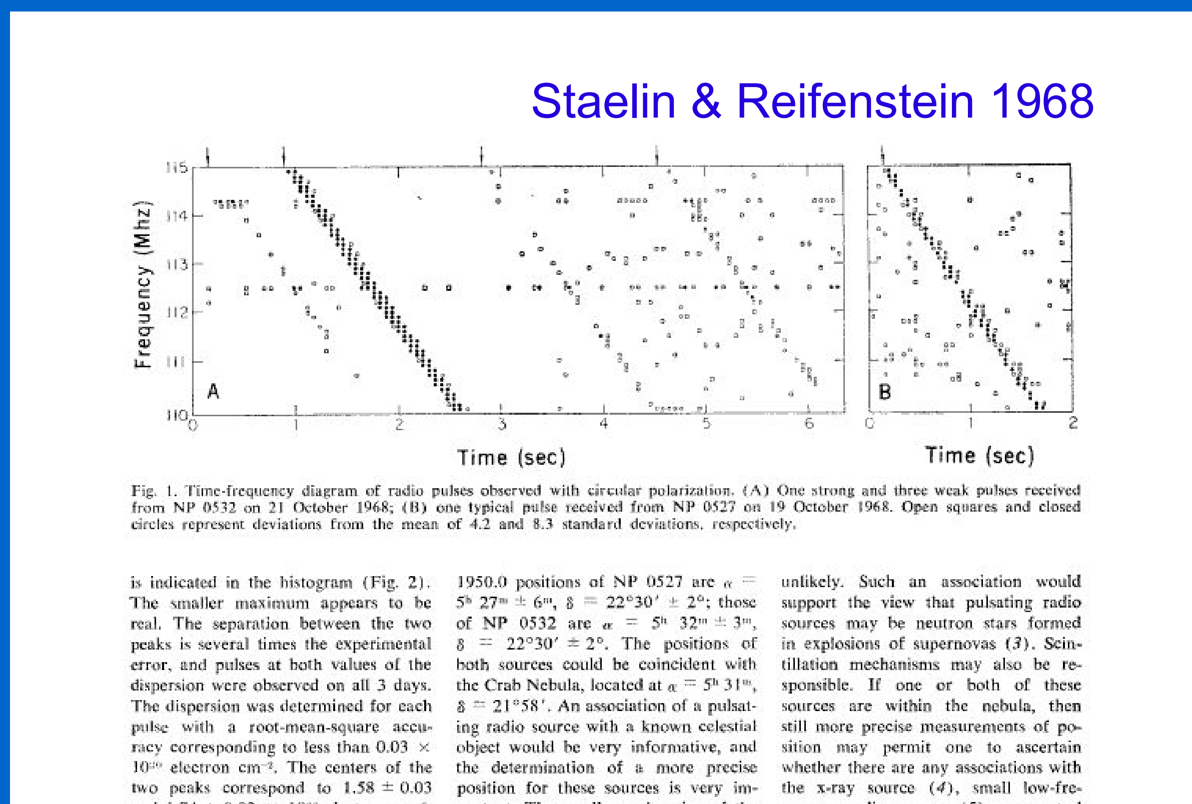
Staelin & Reifenstein 1968

Fig. 1. Time-frequency diagram of radio pulses observed with circular polarization. (A) One strong and three weak pulses received from NP 0532 on 21 October 1968; (B) one typical pulse received from NP 0527 on 19 October 1968. Open squares and closed circles represent deviations from the mean of 4.2 and 8.3 standard deviations, respectively.

is indicated in the histogram (Fig. 2). The smaller maximum appears to be real. The separation between the two peaks is several times the experimental error, and pulses at both values of the dispersion were observed on all 3 days. The dispersion was determined for each pulse with a root-mean-square accuracy corresponding to less than 0.03 × 10^{20} electron cm^{-2}. The centers of the two peaks correspond to 1.58 ± 0.03

1950.0 positions of NP 0527 are $\alpha = 5^h 27^m \pm 6^m$, $\delta = 22°30' \pm 2°$; those of NP 0532 are $\alpha = 5^h 32^m \pm 3^m$, $\delta = 22°30' \pm 2°$. The positions of both sources could be coincident with the Crab Nebula, located at $\alpha = 5^h 31^m$, $\delta = 21°58'$. An association of a pulsating radio source with a known celestial object would be very informative, and the determination of a more precise position for these sources is very im-

unlikely. Such an association would support the view that pulsating radio sources may be neutron stars formed in explosions of supernovas (3). Scintillation mechanisms may also be responsible. If one or both of these sources are within the nebula, then still more precise measurements of position may permit one to ascertain whether there are any associations with the x-ray source (4), small low-fre-

Possible origin of HFCs

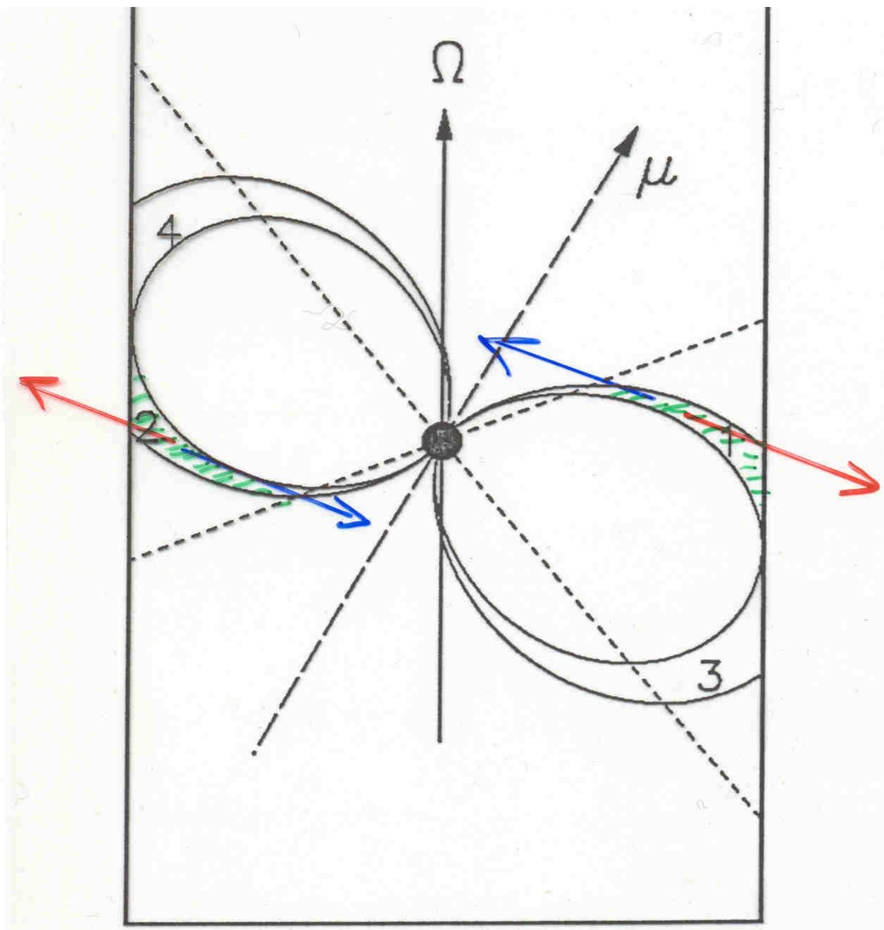

FIG. 1. Schematic illustration of the outer gaps of a pulsar. The outer gap extends from the null charge surfaces (*dashed lines*) to the light cylinder. The value r_{in} is the distance from the star to the intersection between the null charge surfaces of gap 1(2) and the first open field lines.

OUTWARD EMISSION

INWARD EMISSION

(ASSUMED MUCH WEAKER

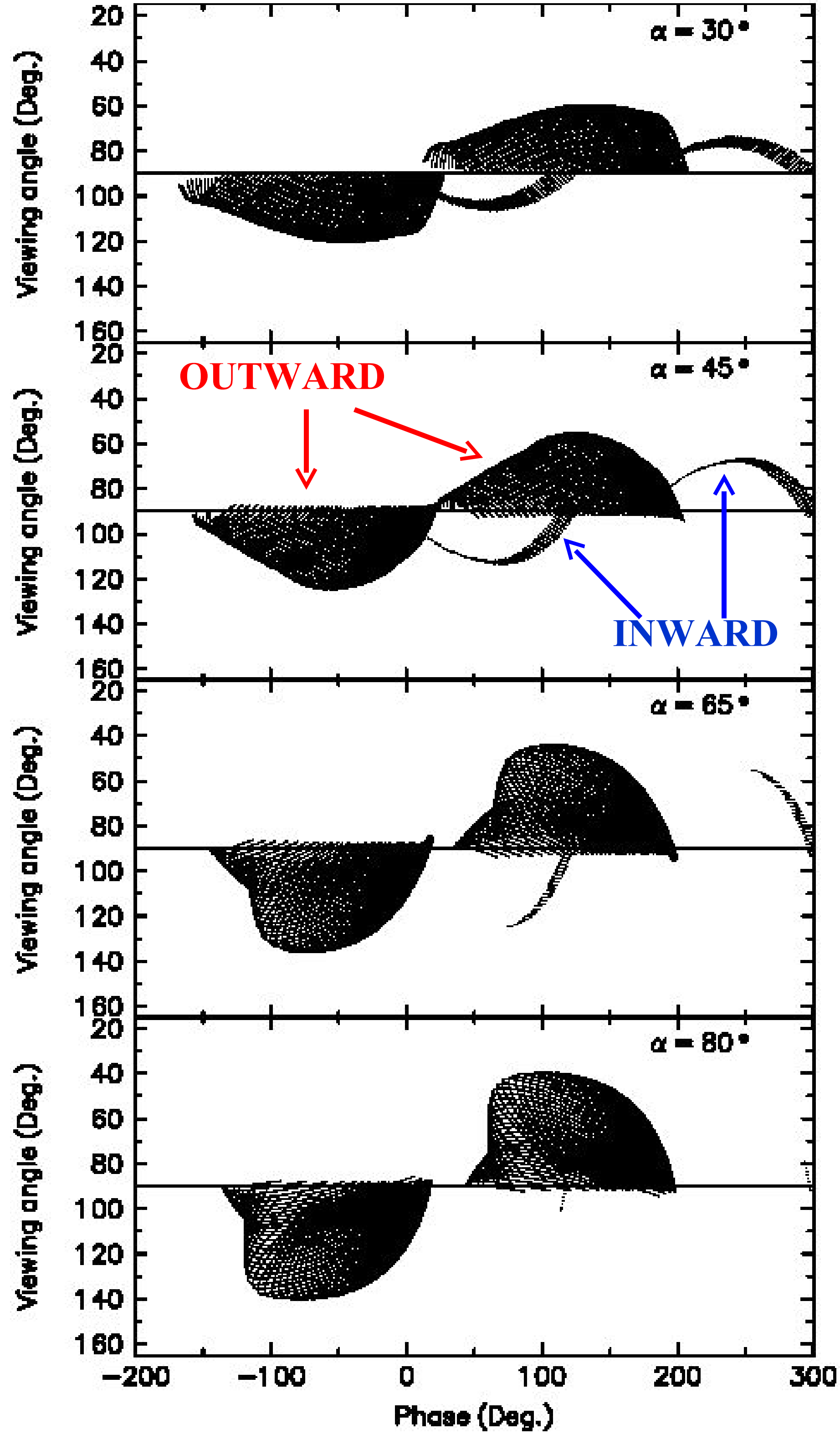

Cheng, Ruderman & Zhang, 2000

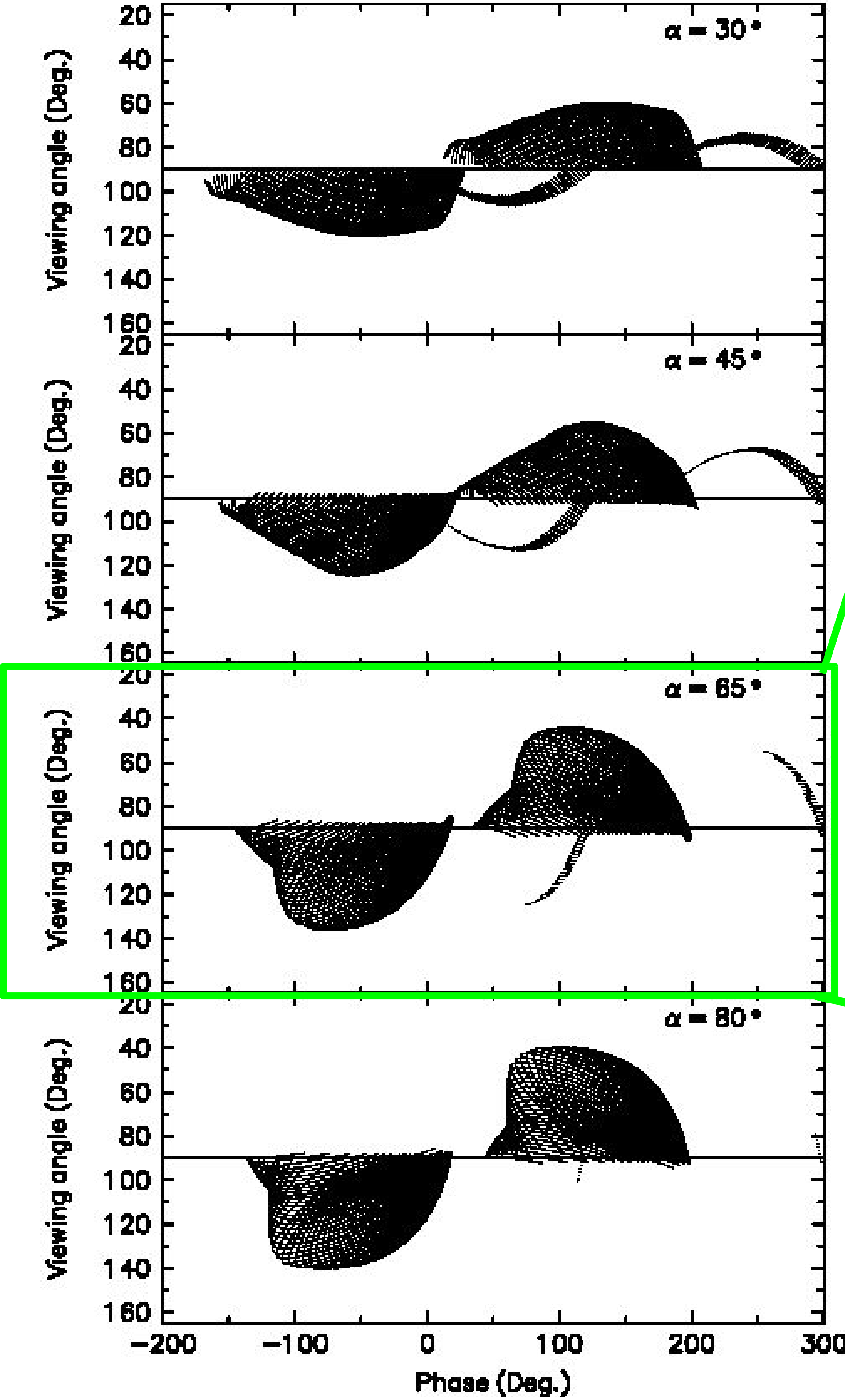

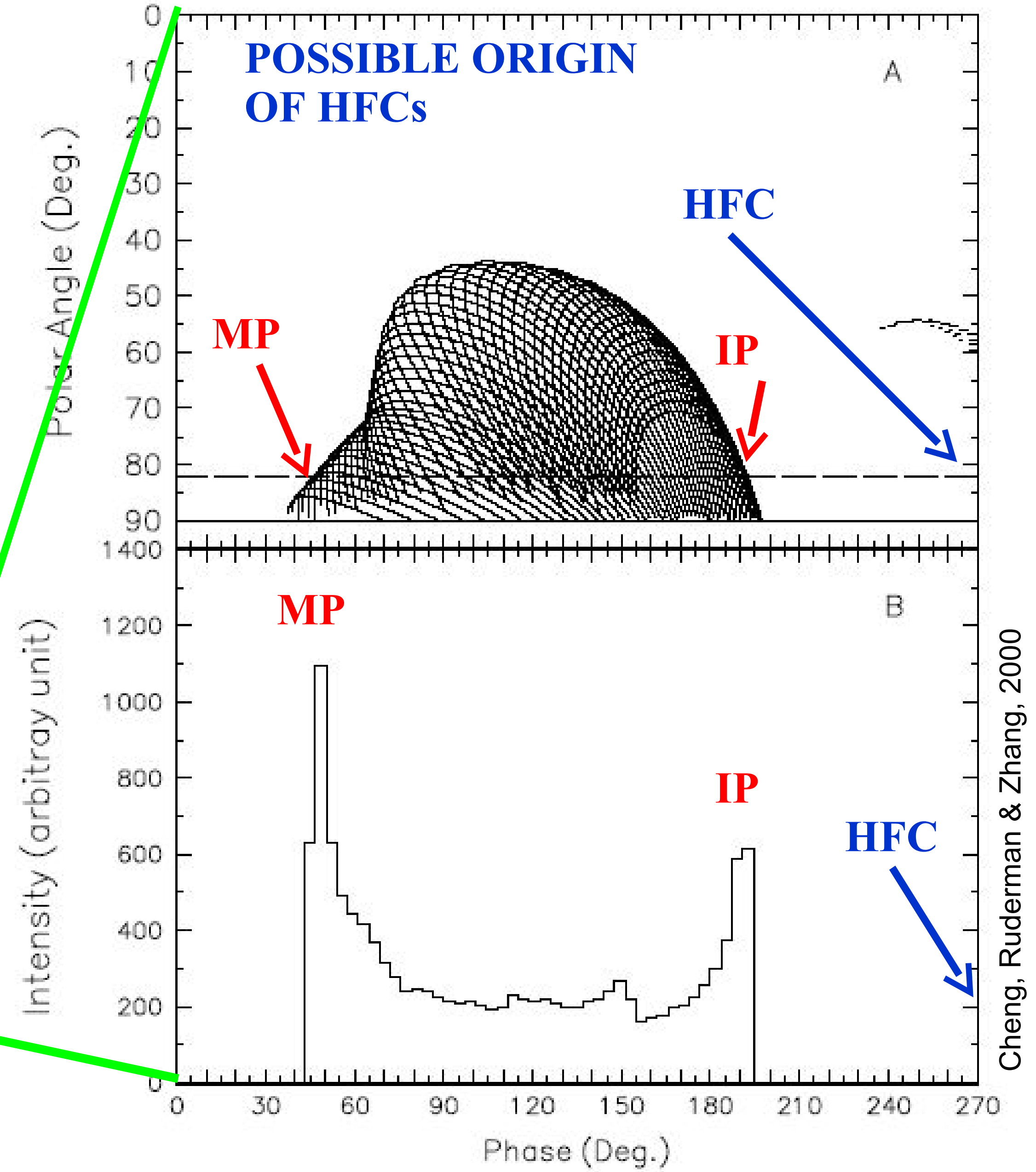

FIG. 8.—Emission projection onto the (ζ, Φ)-plane and pulse profile. The emission consists of the emission outward from both outer gaps and inward only from the region ($r_{\rm lim}$–$r_{\rm in}$) of both outer gaps. The outer gaps are limited along the azimuthal direction by pair production. (*a*) The emission projection ($a_1 = 0.9$) and (*b*) corresponding pulse profile ($\Delta a_1 = 0.03$). Crab parameters, $\alpha = 65°$, $\zeta = 82°$, and $\delta\phi = 150°$, are used.

Enhanced Optical Emission During Crab Giant Radio Pulses

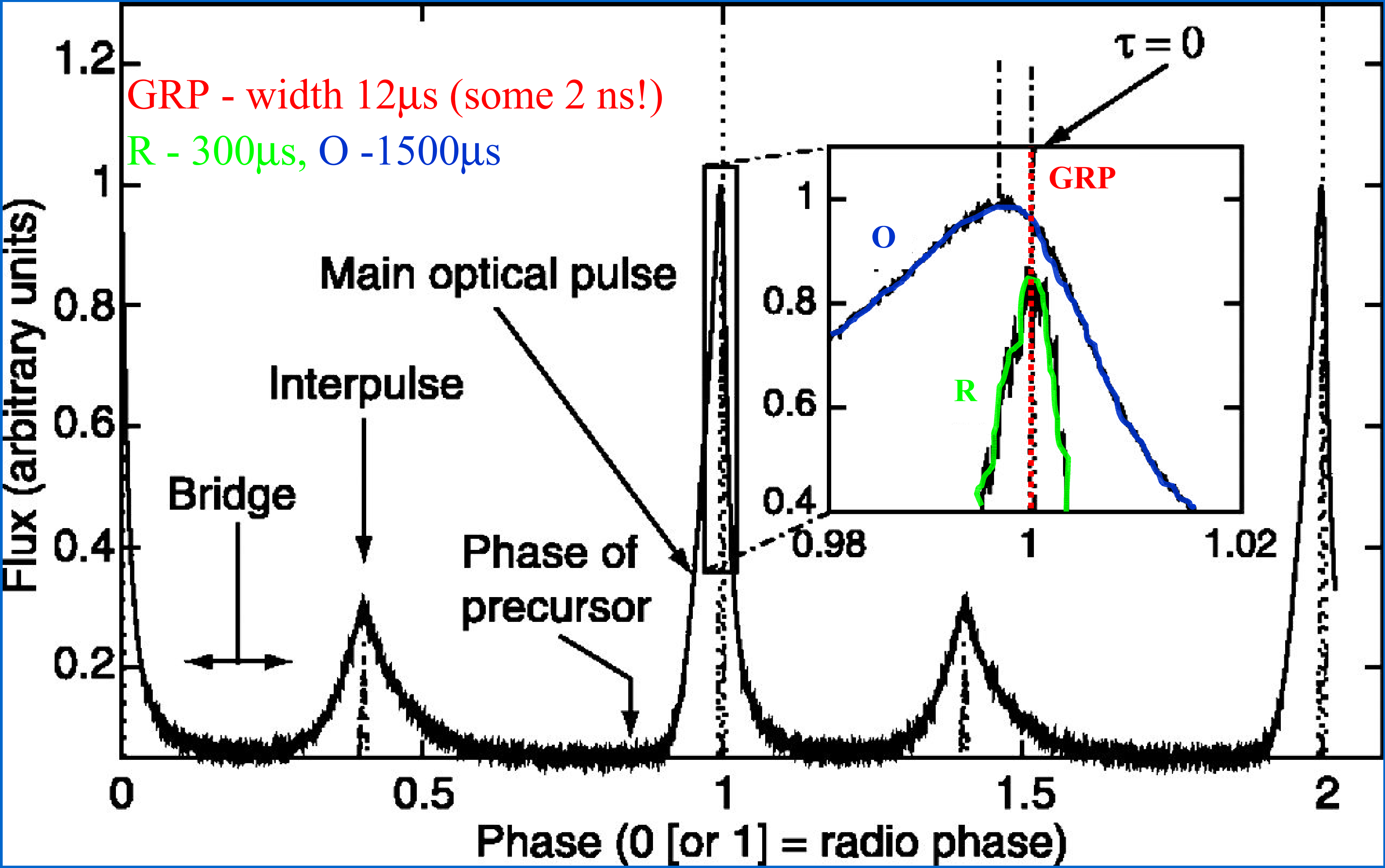

Shearer et al., 2003

The mean optical *giant* pulse in comparison to the average optical pulse

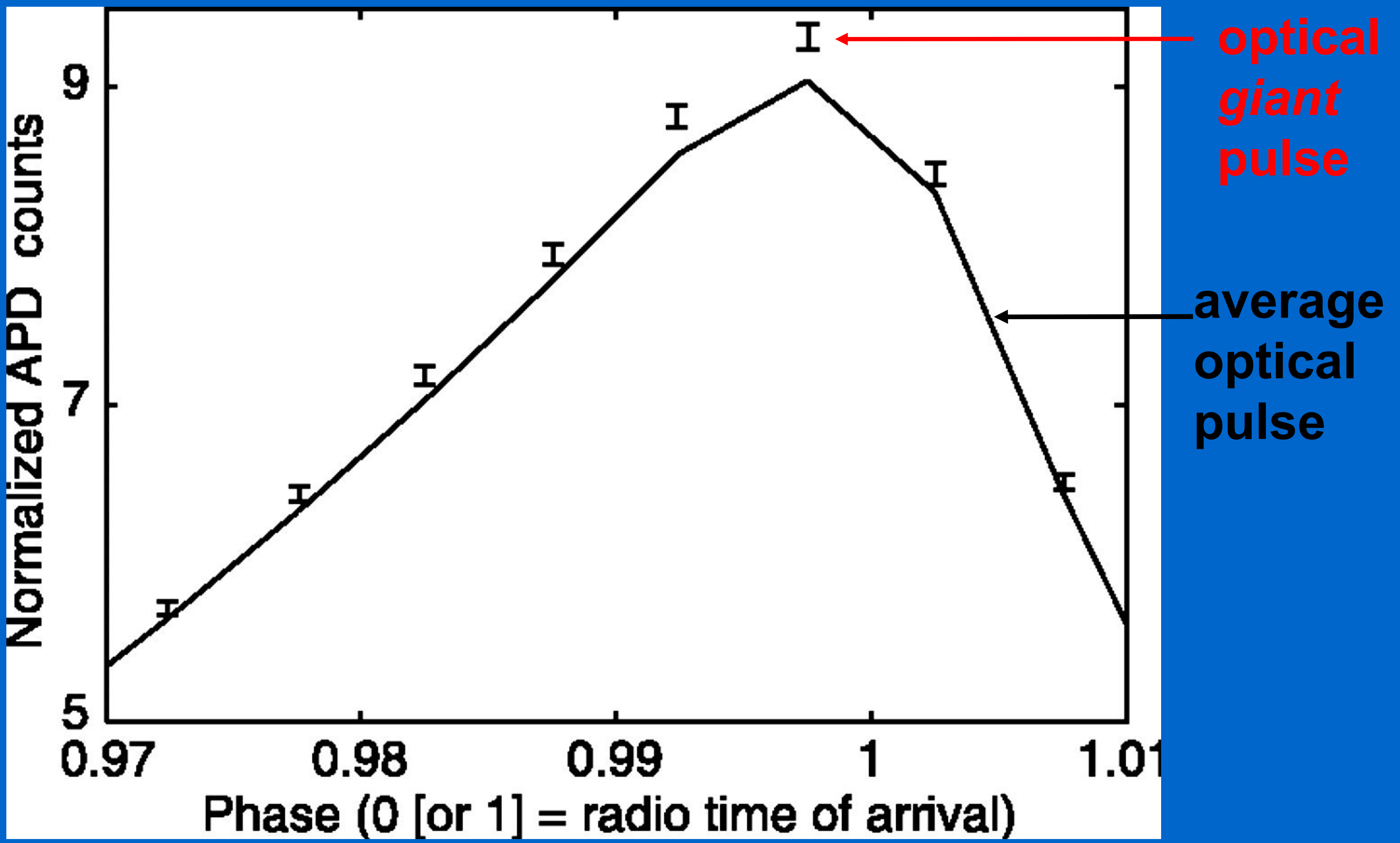

Shearer et al., 2003

The link between optical pulse size and GRP energy

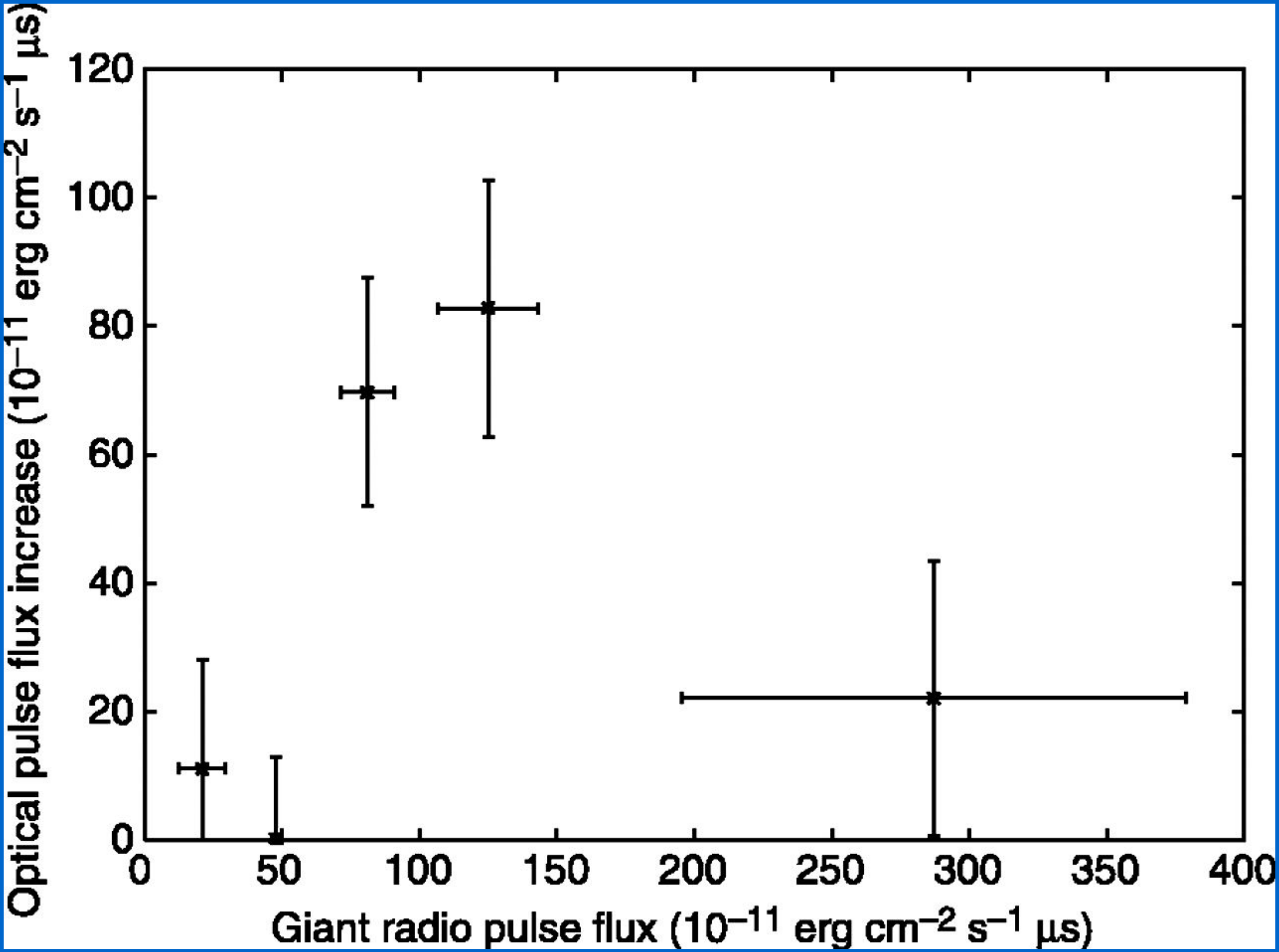

Shearer et al., 2003

Peak strength distribution

0.43 GHz	–2.3	MP
8.8 GHz	-2.9	IP
0.146 GHz	–2.5	MP
0.146 GHz	–2.8	IP
0.812 GHz	-3.6 (all)	